Autoregulation of Ribosome Biosynthesis by a Translational Response in Fission Yeast

François Bachand,[1]* Daniel H. Lackner,[2] Jürg Bähler,[2] and Pamela A. Silver[3]

Department of Biochemistry, Université de Sherbrooke, Sherbrooke, Québec, Canada[1]; Wellcome Trust Sanger Institute, Hinxton, Cambridge CB10 1SA, United Kingdom[2]; and Department of Systems Biology, Harvard Medical School and Dana Farber Cancer Institute, Boston, Massachusetts[3]

Maintaining the appropriate balance between the small and large ribosomal subunits is critical for translation and cell growth. We previously identified the 40S ribosomal protein S2 (rpS2) as a substrate of the protein arginine methyltransferase 3 (RMT3) and reported a misregulation of the 40S/60S ratio in *rmt3* deletion mutants of *Schizosaccharomyces pombe*. For this study, using DNA microarrays, we have investigated the genome-wide biological response of *rmt3*-null cells to this ribosomal subunit imbalance. Whereas little change was observed at the transcriptional level, a number of genes showed significant alterations in their polysomal-to-monosomal ratios in *rmt3Δ* mutants. Importantly, nearly all of the 40S ribosomal protein-encoding mRNAs showed increased ribosome density in *rmt3* disruptants. Sucrose gradient analysis also revealed that the ribosomal subunit imbalance detected in *rmt3*-null cells is due to a deficit in small-subunit levels and can be rescued by rpS2 overexpression. Our results indicate that *rmt3*-null fission yeast compensate for the reduced levels of small ribosomal subunits by increasing the ribosome density, and likely the translation efficiency, of 40S ribosomal protein-encoding mRNAs. Our findings support the existence of autoregulatory mechanisms that control ribosome biosynthesis and translation as an important layer of gene regulation.

The posttranslational modification of proteins is one way that cells extend the chemical diversity of polypeptides beyond the constraints of the encoded amino acids. Protein methylation has emerged as a covalent modification important for the regulation of cell growth and differentiation. Protein arginine methyltransferases (PRMT) use *S*-adenosylmethionine as a methyl donor to catalytically modify proteins by the addition of monomethyl groups onto the guanido nitrogen atom of the arginine side chain (5). PRMTs are divided into two classes depending on the type of dimethylarginine they generate (asymmetric [type I] or symmetric [type II]) (5). Cellular proteins harboring asymmetric and/or symmetric dimethylarginines have been identified through a variety of genetic and biochemical approaches (9, 21, 38). Many of the proteins modified by arginine methylation are involved in binding nucleic acids (17). Interestingly, a proteomic survey of Golgi-associated proteins identified several arginine-methylated polypeptides (61), suggesting a broad spectrum of cellular functions for substrates of arginine methylation.

PRMTs are specific to eukaryotes and are evolutionarily conserved. This protein family presently includes eight vertebrate members, several of which show strong homology to gene products from other eukaryotic species, such as yeast, flies, and worms (8). Although the biological roles of PRMTs remain unclear, they have been associated with a variety of cellular functions, such as transcriptional response (12, 28), mRNA biogenesis and export (48, 65), DNA repair (10), and ribosome biosynthesis (4). The importance of PRMTs during the development of multicellular organisms is further highlighted by the

lethal phenotypes of mice that are genetically engineered for deletion of the *prmt1* (39), *prmt4* (62), and *prmt5* (8) genes.

The ribosome is a large ribonucleoprotein complex assembled from four rRNAs and >80 different ribosomal proteins (RPs). It is estimated that rapidly dividing yeast cells generate new ribosomes at a rate of >2,000/min, accounting for >50% of total cellular transcription (60). Most of the genes associated with ribosome biogenesis are coordinately regulated depending on environmental stresses, nutrient conditions, and developmental stages (11, 13, 18). The coordinate regulation of ribosome biosynthetic factors, especially RP genes, is accomplished at different levels, i.e., the transcriptional (44, 47, 58), posttranscriptional (20), and translational (34) levels. Experimental evidence also suggests that the synthesis and turnover of RPs are controlled to generate equimolar amounts of all RPs (40, 55, 59); however, the underlying mechanisms that balance RP production with subunit assembly remain to be understood. Ribosomal proteins are subject to a variety of posttranslational modifications, including acetylation, ubiquitination, phosphorylation, and methylation (29, 31, 37). The functional role of most of these RP modifications in ribosome function and translational control is still unclear.

We and others have previously identified PRMT3 as an RP methyltransferase (4, 51). *Schizosaccharomyces pombe* cells deleted for the *rmt3* gene (a homolog of mammalian *prmt3*) are depleted of arginine-methylated rpS2 and show an imbalance in the level of small and large ribosomal subunits (4). Ribosome biosynthesis has recently received attention because of its connection with cell size determination (25, 33) and the association between RP gene haploinsufficiency and tumorigenesis (2, 54). Here we have investigated the biological response to the ribosomal subunit misregulation of *rmt3*-null cells (*rmt3Δ* cells) by using DNA microarrays. We report here the transcrip-
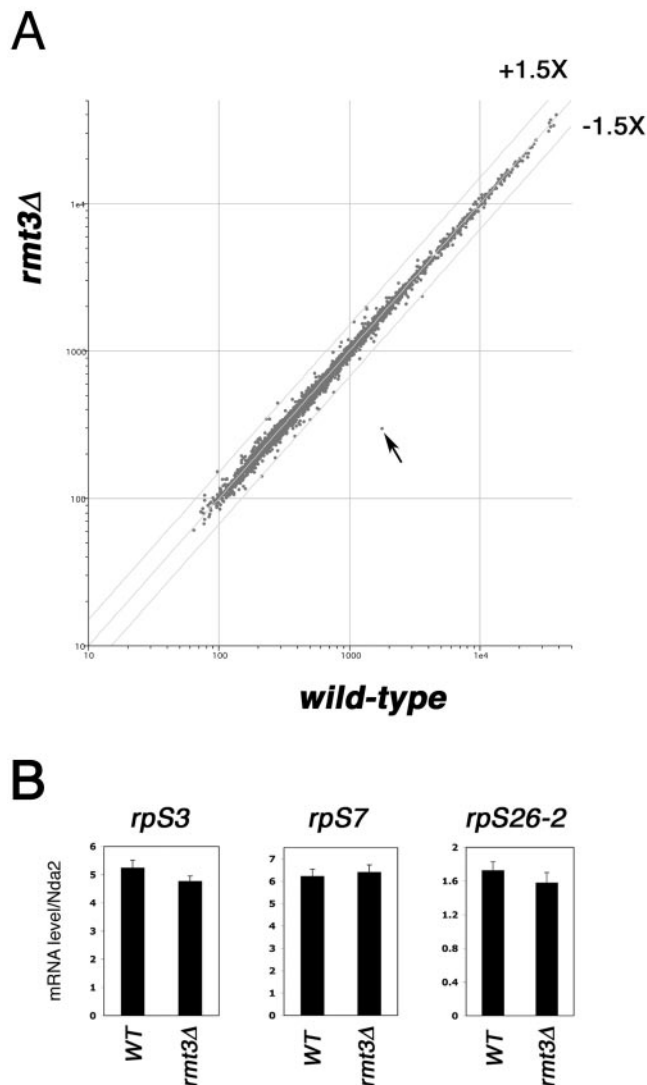
A

B

FIG. 1. Genome-wide mRNA profiling of *rmt3*-null fission yeast cells. (A) Scatter plot of mRNA signals from wild-type (*x* axis) and *rmt3*-null (*y* axis) cells. The scatter plot was generated from averaged data for three independent biological repeats. Dots above the top oblique line represent genes induced >1.5-fold; dots below the bottom oblique line represent genes repressed >1.5-fold. The single gene spot significantly downregulated in *rmt3*Δ cells corresponds to *rmt3* mRNA and is indicated by an arrow. (B) Real-time PCR validation of the genome-wide expression profiling data for three ribosomal protein-encoding genes. mRNA levels for the *rpS3*, *rpS7*, and *rpS26-2* genes were normalized to that of *nda2* mRNA. Error bars were calculated from three independent experiments and represent standard deviations.

tome analysis of *rmt3*Δ cells and the first genome-wide translational profiling study with the fission yeast *S. pombe*. Our data indicate significant changes in the translational activities of several mRNAs in *rmt3*Δ cells, but little variation in overall mRNA abundance. We found that the majority of the 40S RP-encoding mRNAs were redistributed to larger polysomes in *rmt3*-null cells, suggesting enhanced translation efficiency. We also demonstrate that rpS2 overexpression suppressed the ribosomal subunit imbalance seen in *rmt3*Δ cells. Our findings suggest that *rmt3*-null cells respond to the rpS2-dependent small ribosomal subunit deficiency by upregulating the ribosome density of 40S RP mRNAs.

MATERIALS AND METHODS

Yeast cultures and plasmid construction. The use and generation of *rmt3*-null fission yeast were described previously (4). Cells were grown at 30°C in yeast extract medium supplemented with the appropriate amino acids. cDNAs carrying the *rpS2*, *rpS3*, and *rpS7* genes plus upstream regulatory sequences were amplified by PCR from fission yeast genomic DNA, using the following primer sets: for *rpS2*, the 5′ primer AAACTGCAGGGGACTGTCGATGCAAAC ATGAC and the 3′ primer CGCGGATCCTTACTTGTCGTCATCGTCTTT GTAATCGTACTTCTTCTCAGTTTGCATC; for *rpS3*, the 5′ primer AAA CTGCAGATGCGCATTCTTGGATAAAGACA and the 3′ primer CGCGGA TCCTTACTTGTCGTCATCGTCTTTGTAATCGTAAGCAACAGCAGTCTC TTGTTC; and for *rpS7*, the 5′ primer AAACTGCAGGAAAGATGCACTATG TGATGCCT and the 3′ primer CGCGGATCCTTACTTGTCGTCATCGTCTTT GTAATCCAAGCCCTCGCCGGTAGCAACAG. The 5′ primers contained PstI sites, whereas the 3′ primers contained BamHI sites and the DNA sequence coding for the FLAG epitope. The PstI-BamHI-digested PCR products were ligated to pREP3X and pREP4X vector backbones previously digested with PstI and BamHI. This cloning strategy removed the *nmt1* promoter from the pREP3X and pREP4X vectors and expressed the *rpS2*, *rpS3*, and *rpS7* genes under the control of their endogenous promoters.

cDNA microarray analysis. Total RNA for microarray analysis was obtained from early-log-phase (optical density at 600 nm [OD$_{600}$], 0.2 to 0.4) cells and was prepared as described at http://www.sanger.ac.uk/PostGenomics/S_pombe/. cDNA synthesis, labeling, and microarray hybridization procedures have been described previously (32). Results from microarray hybridization were analyzed using Genepix (Axon Instruments) and GeneSpring (Silicon Genetics) software, and the raw data were filtered and normalized as previously described (32). Analysis of the normalized data was performed with Cluster/TreeView software (15) (available at http://rana.lbl.gov/EisenSoftware.htm) and the Significance Analysis of Microarrays (SAM) program available at http://www-stat.stanford .edu/~tibs/SAM/, as previously described (57). Briefly, SAM provides a statistical value (*d* score) calculated for each gene based on the change in gene expression relative to the standard deviation of repeated measurements. Using the gene set detected in at least two of the three biological repeats between monosomal and polysomal RNAs from wild-type and *rmt3* deletion mutant cells (*n* = 3,389), SAM performed a two-class paired comparison and generated a set of 71 significant genes having *d* scores above the threshold (Δ) level of 2.0 for expected values. At this threshold, the false discovery rate was estimated to be below 0.001% (57).

Polysome analysis and RNA isolation. Polysome profiles were analyzed for extracts of log-phase fission yeast (OD$_{600}$, 0.4 to 0.7) as described previously (4).

FIG. 2. Analysis of translational state of *rmt3*-null cells at the genome-wide level. (A) Fractionated polysome profiles of wild-type (WT) and *rmt3*-null (*rmt3*Δ) extracts were subsequently pooled into monosomal (mono) and polysomal (poly) fractions. Monosomal RNAs isolated from wild-type and *rmt3*Δ cells were converted to labeled cDNAs and competitively hybridized to DNA microarrays; polysomal RNAs isolated from wild-type and *rmt3*Δ cells were processed in the same way. (B) Translational changes in *rmt3*Δ mutant cells. RNAs from monosomal and polysomal fractions from *rmt3*Δ cell extracts were reverse transcribed with Cy5 and directly compared to Cy3-labeled cDNAs from wild-type (WT) monosomal and polysomal fractions, respectively. The results displayed are for three biological repeats (*x* axis). Intensity ratios (*rmt3*Δ/WT) for the mRNAs are plotted on the *y* axis on a log scale. Genes displayed in red (*n* = 59) showed a shift towards polysomal fractions in *rmt3*Δ cells compared to wild-type cells, whereas genes displayed in green (*n* = 12) showed a shift towards monosomal fractions in *rmt3*Δ cells compared to wild-type cells. (C) Genome-wide changes in the polysomal-to-monosomal RNA ratio in *rmt3*Δ cells. Using mean data for the three biological repeats, an *rmt3*Δ mutant/wild-type signal ratio was calculated for each monosomal and polysomal mRNA detected in two of three biological repeats. A scatter plot of the normalized monosomal (*x* axis) and polysomal (*y* axis) RNA signals is shown. Red spots represent genes coding for 40S ribosomal proteins.
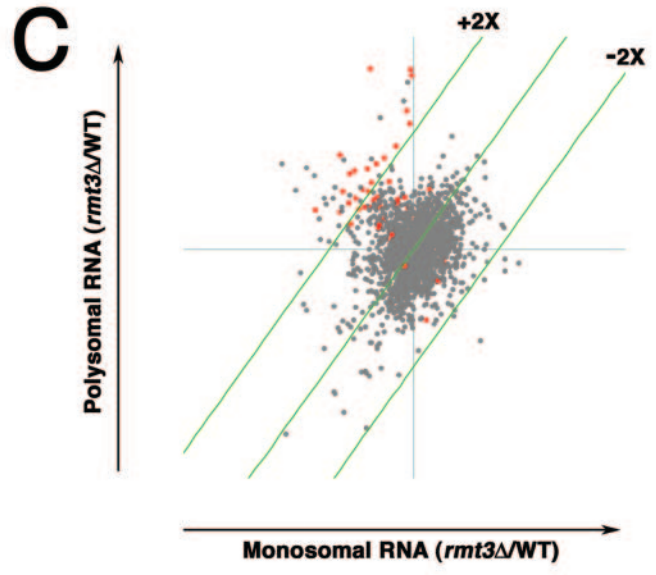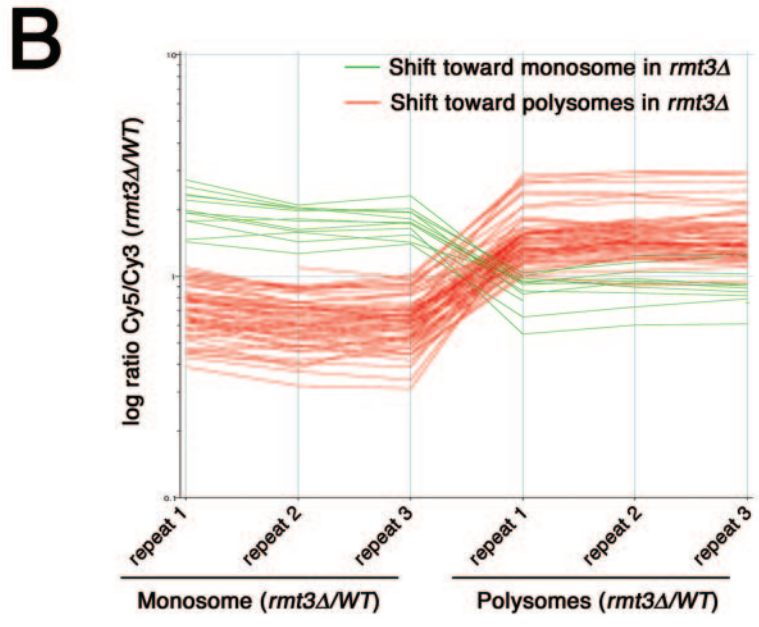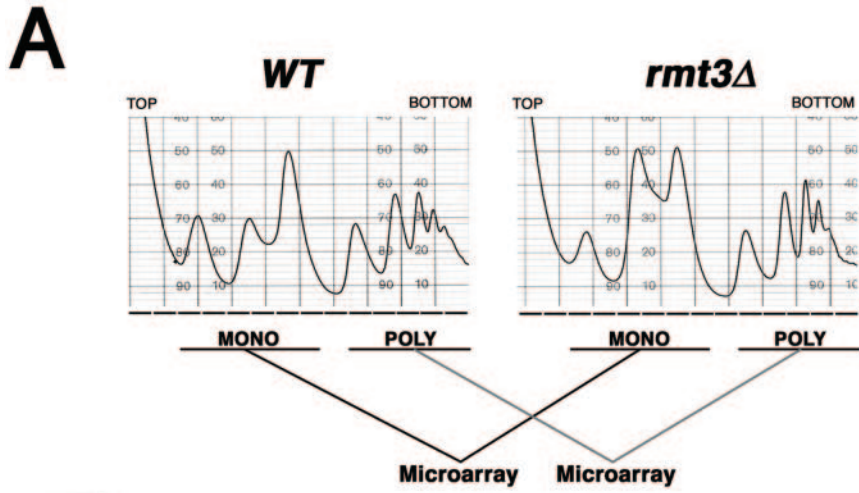
TABLE 1. Genes translationally regulated in *rmt3Δ* cells, as identified by SAM

Gene name and category	Function[a]	SAM score[b]	Fold change P/M[c]	Fold change T[d]	Gene name and category	Function[a]	SAM score[b]	Fold change P/M[c]	Fold change T[d]
Upregulated genes					*rps1-2*	40S ribosomal protein	3.6	1.9	0.9
rps26-2	40S ribosomal protein	12.5	4.2	1.0	*rps0-2*	40S ribosomal protein	3.5	2.0	1.0
rps17-2	40S ribosomal protein	11.6	3.0	1.2	*mcl1*	DNA replication	3.5	2.9	1.0
rps21	40S ribosomal protein	9.6	2.9	1.1	*tif45: tif1*	Translation initiation	3.5	2.3	1.0
SPBC29A3.07c	RNA-binding protein	9.1	2.8	1.0	SPBC3H7.08c	Unknown	3.4	1.9	1.0
rpl29	60S ribosomal protein	8.1	2.9	1.3	*rps1-1*	40S ribosomal protein	3.4	2.0	1.0
rpl39	60S ribosomal protein	7.9	2.6	1.0	*rps15-2*	40S ribosomal protein	3.4	2.2	1.1
nxt2	Nucleocytoplasmic transport	7.6	4.9	1.0	*sui1: psu1*	Translation initiation	3.4	2.3	0.9
SPBC1539.06	Acyl-coenzyme A binding protein	7.1	3.5	1.0	*ckb1*	Casein kinase regulation	3.3	1.7	1.0
rpl44: rpl28	60S ribosomal protein	6.8	3.9	1.0	SPAP27G11.04c	tRNA modification	3.3	2.4	1.0
rps28-2	40S ribosomal protein	6.7	2.4	1.0	SPBC2D10.19c	Unknown	3.3	2.8	1.0
rps29	40S ribosomal protein	6.3	2.2	1.0	*dss1*	Putative proteasome subunit	3.3	1.8	1.0
rps10-2	40S ribosomal protein	6.3	2.6	1.0	*tif6*	Translation initiation	3.2	2.0	1.0
rps19-1	40S ribosomal protein	5.8	2.7	1.0	*rps11-1*	40S ribosomal protein	3.2	2.1	1.0
atp17	Mitochondrial ATPase	5.5	3.8	1.0	SPBC1709.10c	Metal-binding protein	3.2	1.8	1.0
rps23-2	40S ribosomal protein	5.3	3.3	1.1	*eca39*	Aminotransferase	3.2	1.8	1.0
lsm5	snRNA-associated protein	5.1	2.4	1.1	SPBC14C8.04	Acetolactase	3.2	2.7	1.1
rps30-1	40S ribosomal protein	5.1	2.3	1.1	*syb1*	Vesicle transport	3.1	1.8	1.0
SPAC17H9.07	Signal recognition particle	4.8	3.0	1.1	*rps16-1*	40S ribosomal protein	3.1	1.5	1.1
pep1: vps10	Vacuolar transport	4.6	2.7	1.0	*atp1*	Mitochondrial ATPase	3.1	2.0	1.0
rps5	40S ribosomal protein	4.5	2.4	1.0	*rpc19*	DNA-directed RNA polymerase	3.1	1.7	1.1
rps3	40S ribosomal protein	4.5	2.9	1.0	SPCC965.14c	Cytosine deaminase	3.1	1.7	1.4
SPAC1F12.02c	Unknown	4.5	2.0	1.0	SPAC26H5.15	Sterol metabolism	3.0	2.0	0.9
sss1	Endoplasmic reticulum protein translocation	4.4	2.3	1.0					
					Downregulated genes				
rps7	40S ribosomal protein	4.3	2.3	1.1	*pac2*	Sexual development regulation	−6.2	0.5	1.0
rps6-1	40S ribosomal protein	4.3	2.1	0.9	*rpl15-2*	60S ribosomal protein	−5.4	0.4	1.0
rps26-1	40S ribosomal protein	4.2	2.3	1.0	*ura3*	Dihydroorotate dehydrogenase	−4.8	0.3	0.9
sec73	Guanyl-nucleotide exchange	4.2	2.6	1.0	*gpm1*	Gluconeogenesis	−4.8	0.5	1.0
tim17	Mitochondrial protein import	4.1	1.8	1.0	SPAC144.12	Ribose-5-phosphate isomerase	−4.5	0.4	1.0
SPBC83.18c	Unknown	4.1	2.0	1.0	SPBC11G11.03	mRNA decay	−4.3	0.6	1.1
SPAC823.02	Unknown	4.0	1.9	1.0	SPBC8E4.01c	Phosphate transport	−3.9	0.6	1.1
rps9-1	40S ribosomal protein	4.0	2.5	1.0	SPBC2G5.02c	Casein kinase family	−3.8	0.5	1.0
rps5-2	40S ribosomal protein	4.0	2.2	0.9	*pac1*	Double-stranded ribonuclease	−3.8	0.5	1.0
rps9-2	40S ribosomal protein	3.9	1.9	1.1	*eIF3f*	Translation initiation	−3.6	0.6	1.0
cox8	Cytochrome *c* oxidase	3.9	2.3	1.0	SPBC1F3.08c	Unknown	−3.6	0.5	1.1
rpl11-2	60S ribosomal protein	3.7	2.3	1.0	*fib1*	rRNA processing	−3.4	0.5	1.2
rps12-1	40S ribosomal protein	3.6	2.2	1.1					

[a] Gene function was attributed based on GeneDB at http://www.genedb.org/genedb/pombe/indev.jsp.
[b] See Materials and Methods for details.
[c] Fold change in the polysomal/monosomal RNA ratio in *rmt3Δ* cells compared to that in wild-type cells.
[d] Fold change in the total mRNA level in *rmt3Δ* cells compared to that in wild-type cells, as determined by expression profiling.

Sucrose gradients (5 to 45%; prepared without heparin) were centrifuged for 165 min at 35,000 rpm at 4°C in a Beckman SW41 rotor. For microarray analysis, 15 0.8-ml fractions were collected. Fractions 4 to 8 (corresponding to monosomal RNAs) and 11 to 15 (corresponding to polysomal RNAs) from three different gradients were pooled separately in 50-ml conical tubes and precipitated by the addition of 3 volumes of 100% ethanol. Following a 20-min centrifugation at 10,000 rpm at 4°C, each pellet was air dried, resuspended in 1 ml of buffer P (10 mM Tris, pH 7.5, 1 mM EDTA, 0.2% sodium dodecyl sulfate [SDS], 0.8 mg/ml proteinase K), and incubated for 20 min at 37°C. The samples were then extracted with acidic phenol and phenol-chloroform (5:1; pH 4.7) and precipitated with ethanol. The RNA pellets were resuspended in water, quantified using a spectrophotometer, and verified for integrity by gel electrophoresis. Between 10 and 20 μg of monosomal and polysomal RNAs was used for cDNA synthesis and microarray analysis.

For the analysis of mRNA distributions across polysome profiles by real-time PCR, 12 1.0-ml fractions were collected, adjusted to 1% SDS, and stored at −80°C. Following proteinase K treatment, the fractions were extracted with acidic phenol-chloroform (5:1; Sigma), phenol-chloroform-isoamyl alcohol (25:24:1; pH 6.6) (Ambion), and twice with chloroform-isoamyl alcohol. The RNAs were precipitated by the addition of LiCl to a 1.5 M final concentration and 1 volume of isopropanol. The number of ribosomes per mRNA for each fraction was deduced from the ribosomal peaks in the OD$_{254}$ profile (not shown). Each peak in the heavier part of the gradient profile corresponds to an additional ribosome per mRNA.

Real-time PCR. RNA samples (2 μg of total RNA or 5% of the material from a sucrose gradient fraction) were treated with DNase (Invitrogen) and reverse transcribed to cDNAs by using the Taqman reverse transcription reagent (Applied Biosystems). Appropriate dilutions of cDNA were added to SYBR green

PCR master mix (Applied Biosystems) in the presence of a 150 nM concentration (each) of gene-specific primers in 15-μl reaction mixtures. With the exception of duplicated ribosomal protein genes, primer selection was done using Primer Express 2.0 (Applied Biosystems). Applied Biosystems' Prism 7700 sequence detector system was used for real-time PCR amplification and detection. For the calculation of mRNA distributions across polysome profiles, the threshold

TABLE 2. Functional class enrichment of genes with upregulated polysomal/monosomal RNA ratios in *rmt3Δ* cells

Gene ontology class[a]	No. of genes[b]	P value[c]
Eukaryotic 43S preinitiation complex	24	<0.001
Eukaryotic 48S preinitiation complex	24	<0.001
Ribosome	28	<0.001
Protein translation	31	<0.001
Ribonucleoprotein complex (RNP)	29	<0.001
Protein biosynthesis	31	<0.001

[a] Genes identified by SAM (Table 1) as upregulated in their polysomal/monosomal ratio in *rmt3Δ* cells were examined for gene category enrichment within the *S. pombe* Gene Ontology Consortium (3), using FuncAssociate (6).
[b] Number of genes determined by FuncAssociate within each functional gene class.
[c] The significance of enrichment for the listed functional categories was determined by Fisher's exact test, corrected for multiple hypothesis testing, and displayed as a P value.
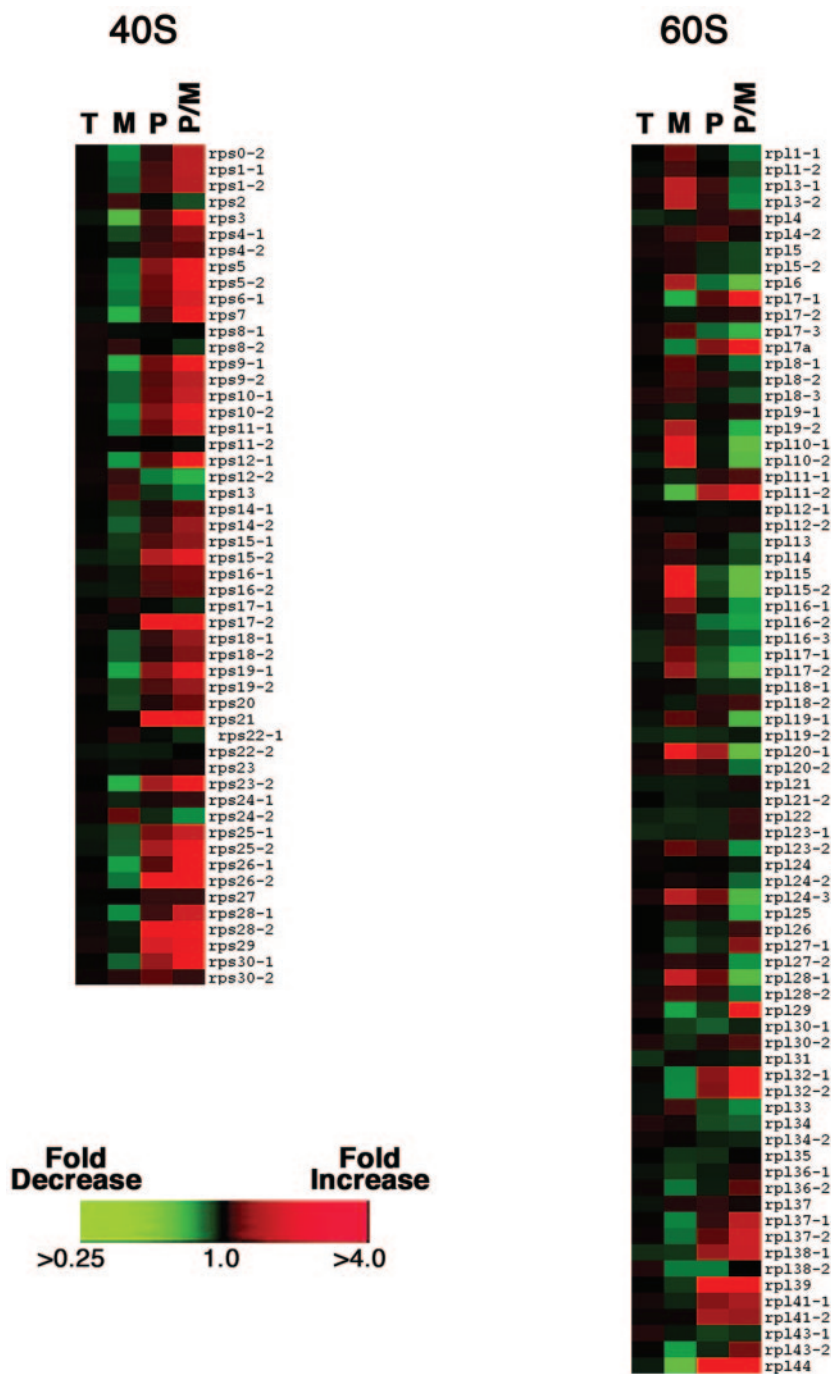
FIG. 3. Gene expression changes of ribosomal protein-encoding mRNAs in *rmt3*-null cells. Each colored square represents the average ratio of total (T), monosomal (M), or polysomal (P) mRNAs isolated from *rmt3*-null cells relative to wild-type cells from three biological repeats. Polysomal-to-monosomal (P/M) RNA ratios are also represented and were calculated based on the average and normalized monosomal and polysomal ratios. Black squares denote no significant alteration in the amount of RNA isolated from *rmt3Δ* or wild-type cells; red and green squares denote ribosomal protein mRNAs that were more or less abundant, respectively. The intensity of the color is proportional to the log$_2$ increase or decrease, as indicated on the intensity scale.

cycle (C_T) of each fraction was subtracted from the C_T of maximum value (always either fraction 1 or 2) for each primer set. The resulting difference in threshold cycles (ΔC_T) was used to calculate the relative change in mRNA levels between fractions by calculating the $2^{\Delta C_T}$ value. The mRNA distribution across the entire polysome profile was graphically presented as the percentage of mRNA in each fraction divided by the total amount of mRNA (sum of 12 fractions).

Protein analysis. Log-phase wild-type and *rmt3Δ* fission yeast cells were resuspended in urea lysis buffer (50 mM sodium phosphate, pH 8.0, 4 M urea, 0.1% Triton X-100, 0.25 M NaCl, 10 mM imidazole, 5 mM β-mercaptoethanol, protease inhibitors) and lysed in Fastprep FP120 (Qbiogene, Inc.), using 0.5-mm glass beads. Clarified lysates were normalized for total protein concentration by using the Bradford protein assay (Bio-Rad, Inc.). Proteins were separated by
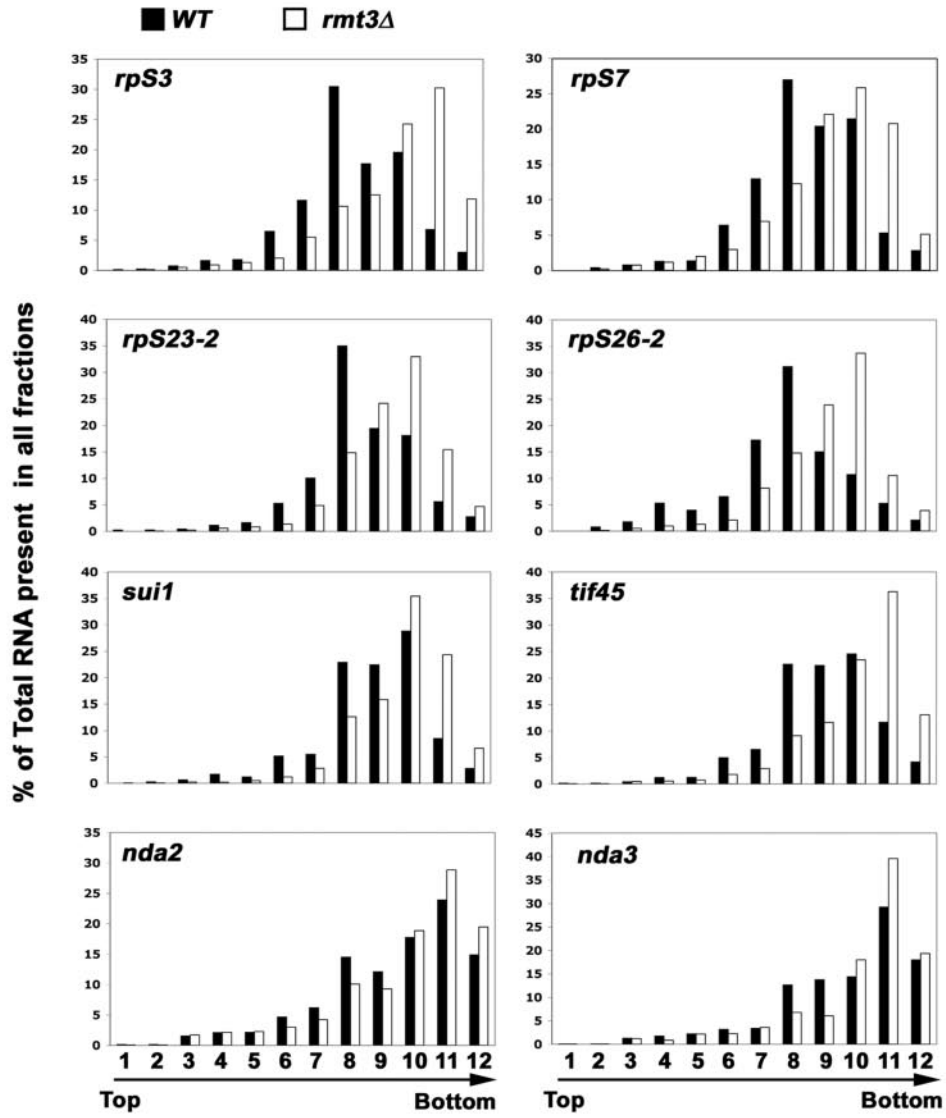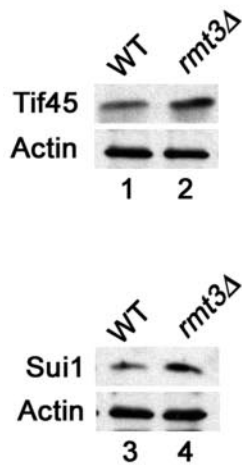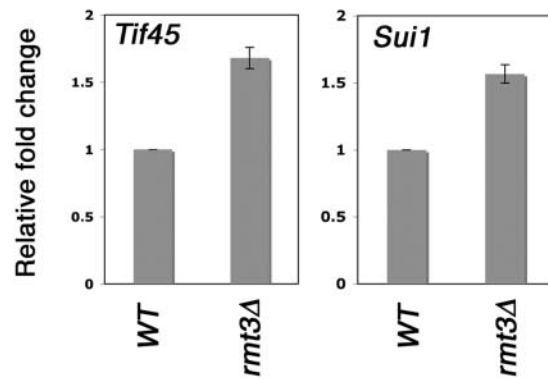
SDS-polyacrylamide gel electrophoresis (SDS-PAGE) (13%) and transferred to nitrocellulose membranes (Schleicher & Schuell). Mouse monoclonal antiactin (Chemicon International), rabbit polyclonal anti-Tif45 (42), and rabbit polyclonal anti-Sui1 (64) were used to probe the membranes. Membranes were then probed with goat anti-rabbit and anti-mouse secondary antibodies conjugated to Alexa fluor 680 (Molecular Probes) and IRdye 800 (Rockland Immunochemicals), respectively. Linear detection of the proteins was performed and quantified using the Odyssey infrared imaging system (LI-COR).

RESULTS

Genome-wide expression profiling of *rmt3Δ* cells. To elucidate the mechanism by which *rmt3*-null cells respond to the imbalance between the levels of small and large ribosomal subunits, steady-state changes at the transcriptional level were examined using DNA microarrays. Total RNAs harvested from *rmt3Δ* cells and an isogenic wild-type strain were reverse transcribed, labeled, and hybridized to microarrays that displayed all of the known and predicted genes in the *S. pombe* genome, as well as some noncoding sequences (32). The overall data analyzed from three independent biological replicates, including a dye-swapping experiment, revealed that the global pattern of gene expression in *rmt3Δ* cells was similar to that in wild-type control cells. As shown in Fig. 1A, *rmt3* was the only gene that consistently demonstrated a >1.5-fold change in gene expression in all three biological repeats. In conclusion, *rmt3Δ* cells demonstrated little change in their global expression signature compared to normal cells. These data show that *rmt3*-null cells do not respond to the ribosomal subunit imbalance by changing the mRNA abundance of genes involved in ribosome function.

Genome-wide translational profiling of *rmt3Δ* cells. Because of the absence of change at the transcriptional level, we next hypothesized that alterations in the spectrum of translated mRNAs may provide a biological response to the ribosomal subunit imbalance in *rmt3Δ* cells. To test this, we examined the translational state of a large number of cellular mRNAs by microarray analysis of monosomal versus polysomal RNAs. Total cellular extracts prepared from wild-type and *rmt3*-null cells were separated in 5% to 45% sucrose gradients and fractionated into 15 different samples. Fractions corresponding to free ribosomal subunits and monosomes (fractions 4 to 9; Fig. 2A) and to polysomes (fractions 11 to 15; Fig. 2A) were pooled, and the corresponding RNAs were isolated. Following conversion of the RNAs to labeled cDNAs, monosomal RNAs from wild-type and *rmt3Δ* cells were competitively hybridized to the *S. pombe* arrays; the polysomal RNAs were processed and analyzed in the same way (Fig. 2A).

According to the hybridization signals obtained from the microarray data, 3,389 genes were detected in at least two of the three biological repeats in both monosomal and polysomal RNA fractions from wild-type and *rmt3*-null cells. Statistical analysis by SAM (see Materials and Methods) was used to identify mRNA species that significantly changed their polysomal-to-monosomal RNA ratios between wild-type and *rmt3Δ* cells. Using a two-class paired comparison, SAM identified 59 upregulated and 12 downregulated mRNAs in *rmt3* deletion mutants (Fig. 2B). The genes identified by SAM are presented in Table 1.

Computational algorithms (3, 6) were used to distinguish functional gene classes within the mRNA species identified by SAM. The analysis identified several functional categories associated with the protein synthesis machinery for the gene set that showed higher polysomal-to-monosomal RNA ratios in *rmt3Δ* cells (Table 2). Significantly, 24 genes coding for small-subunit RPs were among the 59 mRNAs with induced polysome/monosome ratios (Tables 1 and 2). When examined globally, the microarray data revealed that the majority of the 40S RP-encoding mRNAs showed redistribution from the monosomal to the polysomal fraction in *rmt3Δ* cells (Fig. 2C and 3). According to the expression profiling data obtained for *rmt3Δ* cells, the increased ribosome loading of small-subunit RP mRNAs was not a consequence of greater levels of the corresponding transcripts (Fig. 1 and 3). Figure 3 also shows that when both the small and large ribosomal subunits were analyzed, the mRNAs coding for 60S RP did not show the overall increase in ribosome density observed for the 40S RP mRNAs. These data suggest a specific posttranscriptional response toward the 40S ribosomal subunit in *rmt3*-null cells.

Validation of microarray analysis. We used real-time PCR to confirm the redistribution of several of the mRNAs selected from Table 1 across sucrose gradients. The *nda2* and *nda3* mRNAs, coding for the *S. pombe* tubulin alpha-1 and beta chains, respectively, were selected as control genes whose polysomal-to-monosomal ratios did not change, as determined by the microarray analysis. For these experiments, 12 fractions were collected from sucrose gradients and compared for different mRNA levels using gene-specific primers. Because each individual fraction was quantitatively analyzed, this higher-resolution study resulted in a more comprehensive examination of the distribution of specific mRNAs across polysome profiles than the microarray approach, where monosomal and polysomal RNAs were pooled.

Four different small-subunit RP mRNAs were first examined for their distributions across polysome profiles. Figure 4A shows that the levels of the *rpS3*, *rpS7*, *rpS23-2*, and *rpS26-2* mRNAs peaked in fraction 8 for profiles prepared from wild-type cells. This corresponded to a translation efficiency of 2 to

FIG. 4. High-resolution analysis of mRNA distributions across polysome profiles for selected genes and effects on the synthesis of TIF45 and SUI1 proteins. (A) Specific mRNAs selected from Table 1 were quantitatively analyzed over the entire polysomal profile by real-time PCR. The *nda2* and *nda3* genes were selected as control mRNAs whose distribution did not change based on the microarray analysis. Black and white bars represent the percentage of total RNA present in each fraction for wild-type (WT) and *rmt3*-null (*rmt3Δ*) cells, respectively. The data are the averages of two independent biological replicates. (B) Total cell lysates prepared from wild-type (WT; lanes 1 and 3) and *rmt3*-null (*rmt3Δ*; lanes 2 and 4) cells were resolved by SDS-PAGE on 13% gels, transferred to nitrocellulose membranes, and immunoblotted simultaneously with both mouse antiactin and rabbit anti-Tif45 (top panel) or mouse antiactin and rabbit anti-Sui1 (bottom panel). Membranes were then probed with different fluorescently coupled secondary antibodies (see Materials and Methods) and detected using the Odyssey infrared imaging system (LI-COR). (C) Tif45 and Sui1 protein levels were normalized to the actin signal, using Odyssey quantification software. The obtained protein ratios were then normalized to wild-type (WT) levels. The results represent the averages of three independent biological repeats.

3 ribosomes/mRNA according to the polysome profiles (see Materials and Methods for details). This is in contrast to a density of 4 to 6 ribosomes/mRNA for the same transcripts in *rmt3*-null cells (Fig. 4A, peaks in fractions 10 and 11), suggesting a 50% increase in the translation rates of these transcripts. Three translation initiation factors were also among the genes that showed upregulated polysomal/monosomal ratios in *rmt3Δ* cells (Table 1). Two of these, *sui1* and *tif45-1*, were analyzed for their distributions across sucrose gradients by real-time PCR. Consistent with the microarray data, the mRNAs coding for Sui1 and Tif45 were redistributed to heavier polysomal fractions in *rmt3Δ* cells than in wild-type cells (Fig. 4A). In contrast, the nonribosomal *nda2* and *nda3* genes showed similar distributions across both polysome profiles. Several genes were also verified for their expression levels in wild-type and *rmt3*-null cells. Consistent with the transcription profiling data, the levels of three mRNAs coding for small-subunit RPs were not altered by the deletion of the *rmt3* gene (Fig. 1B).

The aforementioned results indicating a shift to heavier polysomes could be the consequence of more efficient initiation rates or slower elongation kinetics. To distinguish between these two stages of translation, we determined the protein levels of the Tif45 and Sui1 initiation factors, whose mRNAs were redistributed to heavier polysomes in *rmt3*-null cells (Table 1 and Fig. 4A). Total cellular extracts prepared from wild-type and *rmt3Δ* cells were analyzed by immunoblotting using antibodies directed against Tif45 and Sui1, and the expression levels were normalized to actin levels (Fig. 4B). Actin protein levels were used as an internal control in these experiments because it was found that the *act1* mRNA profile did not change in microarray and real-time PCR analyses (data not shown). The results of several immunoblots are quantified in Fig. 4C and indicate higher levels of Tif45 and Sui1 proteins in *rmt3* deletion mutants than in wild-type fission yeast. In conclusion, the data presented in Fig. 4 corroborate the microarray data revealing an increase in ribosome loading of several mRNA species in *rmt3*-null cells. Our results also indicate elevated protein synthesis for two of the genes showing increased polysome association in *rmt3Δ* cells, consistent with enhanced translation initiation rates for these mRNAs.

The ribosomal subunit imbalance of *rmt3*-null cells is caused by a small-subunit deficit and can be rescued by rpS2 overexpression. Given the decrease in the 40S/60S ratio detected in *rmt3Δ* cells (4), the coordinate upregulation in the ribosome density of 40S RP mRNAs in this mutant (Fig. 2 to 4) would be consistent with a biological response to a small-subunit deficiency. To test this hypothesis, we compared sucrose gradient profiles of extracts prepared from wild-type and *rmt3Δ* mutant fission yeast. Deletion of the *rmt3* gene resulted in a ribosomal subunit imbalance that was consistently demonstrated by deficits in the level of small subunits (Fig. 5A). The reduction of 40S ribosomal subunits in *rmt3*-null cells led to the accumulation of free 60S ribosomal subunits (Fig. 5A), consistent with the profiles detected for previously reported mutants defective in small-subunit levels (24, 26, 30, 45).

RMT3 posttranslationally modifies the 40S ribosomal protein S2 by arginine methylation in fission yeast and mammals (4, 51). To test the possibility that the ribosomal subunit imbalance observed in *rmt3*-null cells is dependent on rpS2 function, we examined whether overexpression of rpS2 would alle-

viate the altered polysome profile of *rmt3Δ* cells. A plasmid expressing C-terminal FLAG-tagged rpS2 from its endogenous promoter was transformed, along with a vector control, into wild-type and *rmt3Δ* cells. The rpS2-FLAG protein was incorporated into ribosomes and arginine methylated in an *rmt3*-dependent manner (data not shown), indicating that the plasmid-expressed ribosomal protein was functional. As demonstrated in Fig. 5B, the polysome profile for *rmt3*-null cells transformed with the vector control exhibited an enlarged free 60S ribosomal peak and reduced levels of free small subunits (bottom panel, gray profile). In contrast, an increased dosage of rpS2 in *rmt3Δ* cells consistently reestablished the equilibrium between free 40S and 60S ribosomal subunits (bottom panel, black profile), similar to the case in wild-type fission yeast (top panel). Restoration of the altered ribosomal profile of *rmt3*-null cells was specific to rpS2, as the expression of two different 40S ribosomal proteins, rpS3 and rpS7, did not reestablish the equilibrium between free 40S and 60S subunits (Fig. 5C and D). These results indicate that *rmt3* deletion mutants have reduced levels of the 40S ribosomal subunit and that the molecular events leading to the ribosomal subunit imbalance of *rmt3*-null cells are mediated through the 40S ribosomal protein S2.

Because the overexpression of rpS2 rescued the decrease in 40S ribosomal subunit levels (Fig. 5B), we tested whether rpS2 expression also restored the increased ribosome density of 40S RP mRNAs detected in *rmt3*-null cells (Fig. 3 and 4). Real-time PCRs were used to examine the distributions of the *rpS23-2* and *rpS26-2* small-subunit mRNAs across polysome profiles. Consistent with the results presented in Fig. 4A, *rpS23-2* and *rpS26-2* mRNA levels peaked in fraction 10 in profiles prepared from *rmt3*-null cells previously transformed with the vector control (Fig. 6A and B). The expression of rpS2 (Fig. 6A), but not rpS3 (Fig. 6B), reduced the ribosome densities of the *rpS23-2* and *rpS26-2* mRNAs to levels similar to those detected in normal fission yeast (Fig. 4A). The results presented in Fig. 5 and 6 strongly suggest that the translational upregulation of 40S RP mRNAs is a response to the reduced levels of the 40S ribosomal subunit detected in *rmt3*-null cells.

DISCUSSION

For the present study, genome-wide analyses were performed with cells deleted for the ribosomal protein methyltransferase gene *rmt3*, uncovering a posttranscriptional response to the ribosomal subunit imbalance detected in these cells. We showed that the number of ribosomes per transcript for the majority of the small RP mRNAs significantly increased in *rmt3*-null cells. Importantly, we have shown using expression profiling and real-time PCR that the increased ribosome loading of 40S RP mRNAs in *rmt3Δ* cells is not due to elevated mRNA levels from these genes. Our data also demonstrated that the levels of small ribosomal subunits are reduced in *rmt3Δ* cells and that the consequent 40S-60S imbalance can be rescued by the overexpression of rpS2. The results presented here suggest a case of autoregulation in which *rmt3*-null cells compensate for the reduced amounts of small subunits by increasing the translational activity of mRNAs coding for 40S RPs. To our knowledge, autoregulation of ribosome synthesis by a translational response has not been previously reported. These findings help to elucidate the cellular mechanisms co-
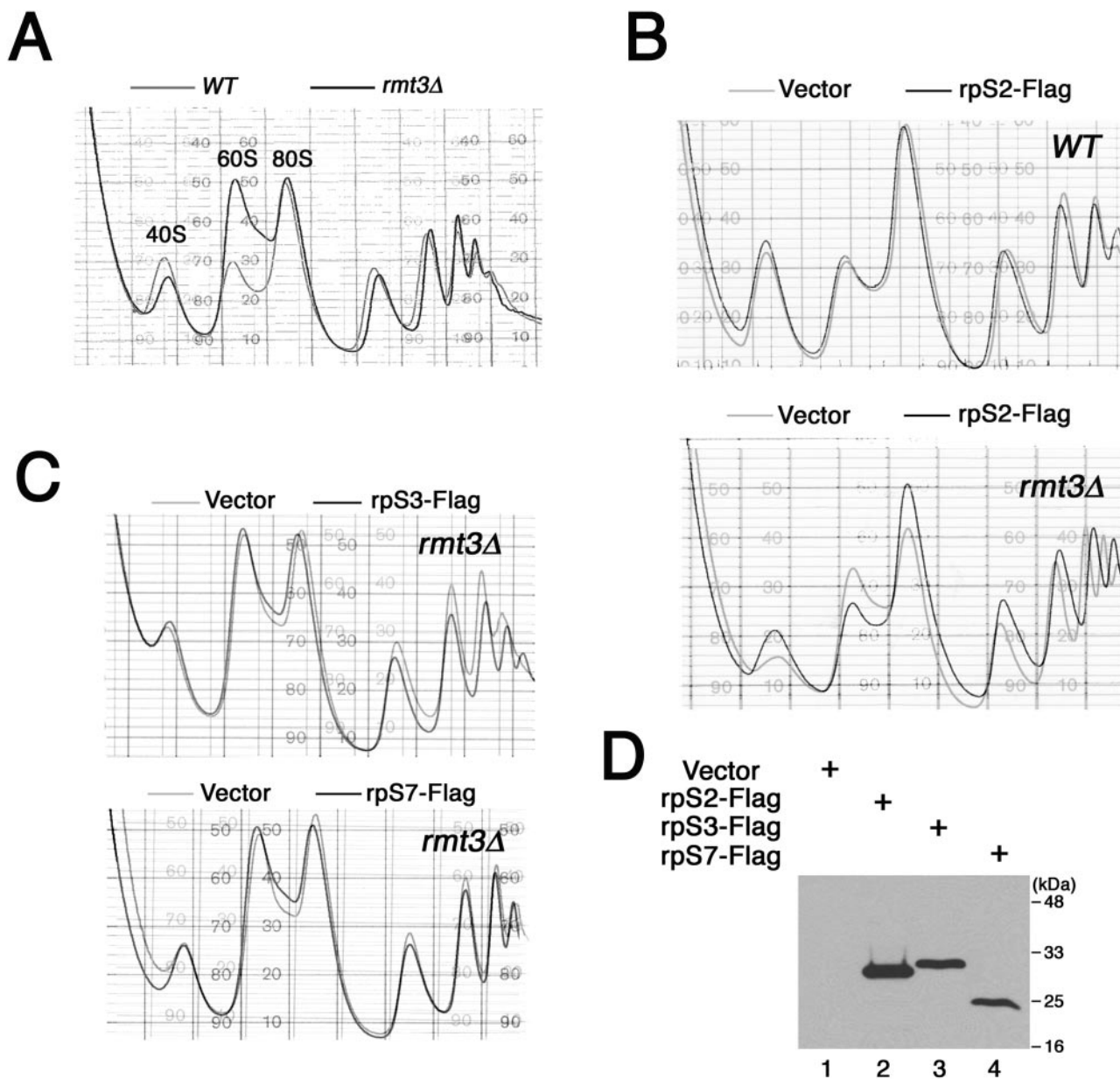
FIG. 5. The ribosomal subunit imbalance of *rmt3*-null cells is caused by a small-subunit deficit and can be rescued by rpS2 overexpression. (A) Sucrose gradient analysis of 25 A_{254} units from extracts prepared from wild-type (gray line) and *rmt3*-null (black line) fission yeast. Small (40S) and large (60S) ribosomal subunits as well as 80S monosomes are indicated. (B) Sucrose gradient analysis of 25 A_{254} units from extracts prepared from wild-type (WT; top panel) and *rmt3*-null (*rmt3Δ*; bottom panel) fission yeast previously transformed with an empty vector control (gray line) or a vector expressing a C-terminal FLAG-tagged rpS2 protein (black line). (C) Sucrose gradient analysis of 25 A_{254} units from extracts prepared from *rmt3*-null fission yeast previously transformed with an empty vector control (gray lines; top and bottom panels) or a vector expressing a C-terminal FLAG-tagged rpS3 (black line; top panel) or FLAG-tagged rpS7 (black line; bottom panel) protein. (D) Total cell lysates prepared from *rmt3*-null cells previously transformed with an empty vector control (lane 1) or vectors expressing C-terminal FLAG-tagged versions of rpS2 (lane 2), rpS3 (lane 3), and rpS7 (lane 4) were resolved by SDS-PAGE on 12% gels, transferred to nitrocellulose membranes, and immunoblotted with an affinity-purified FLAG antibody. Molecular size standards are indicated on the right, in kilodaltons.

ordinating RP production with ribosomal subunit assembly in eukaryotes.

Regulatory networks of ribosome biosynthesis. Ribosomal subunit homeostasis is an integral part of actively dividing cells and is regulated at multiple levels (14, 60). Our results describe

a translational response that compensates for the reduced levels of small ribosomal subunits in *rmt3* deletion mutants; yet, an imbalance of the 40S/60S ratio persists in these cells (4) (Fig. 5). It is estimated that normal yeast cells contain approximately 200,000 ribosomes and 15,000 mRNAs (60). However,
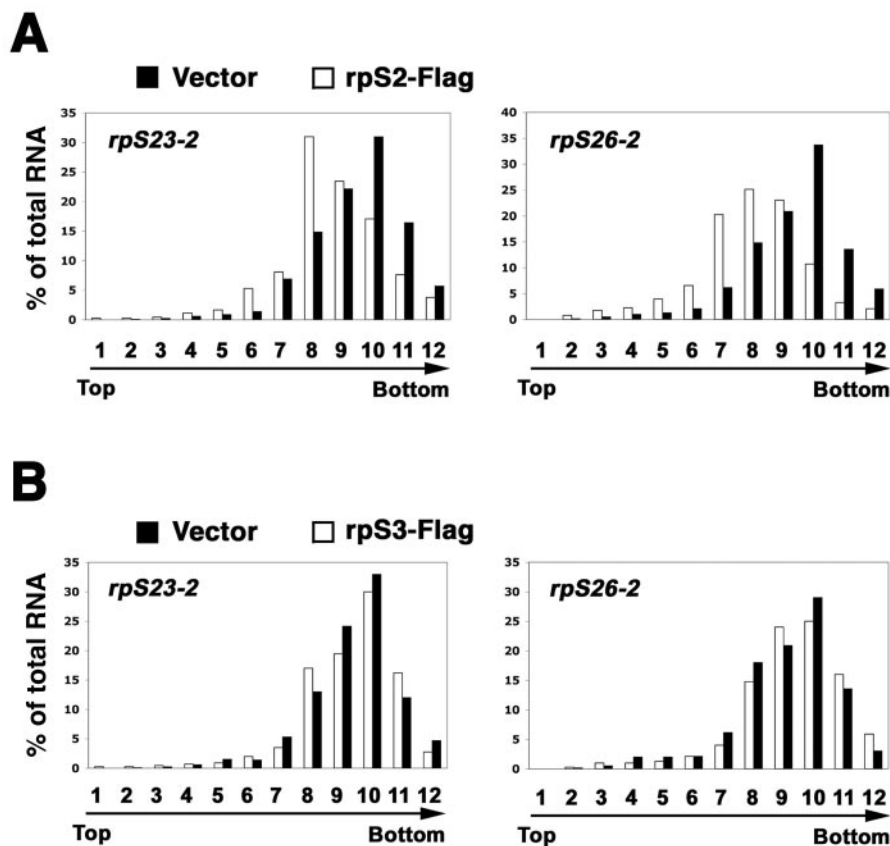
A

B

FIG. 6. Expression of rpS2 restores ribosome densities of *rpS23-2* and *rpS26-2* mRNAs to wild-type levels. *rpS23-2* and *rpS26-2* mRNAs were quantitatively analyzed over the entire polysomal profile by real-time PCR. (A) Bar graphs representing the percentage of total RNA present in each fraction for *rmt3*-null cells previously transformed with a vector control (black bars) or a vector expressing rpS2-Flag (white bars). (B) Bar graphs representing the percentage of total RNA present in each fraction for *rmt3*-null cells previously transformed with a vector control (black bars) or a vector expressing rpS3-Flag (white bars). The data are the averages of two independent biological replicates.

the limiting number of ribosomes sufficient to permit normal cell growth and division is still unclear. Because the growth rate of *rmt3*-null cells is comparable to that of wild-type fission yeast, the redistribution of 40S RP mRNAs to heavier polysomes described here could provide a sufficient number of small ribosomal subunits and functional ribosomes to accommodate global protein synthesis and survival in the mutant. This idea would be consistent with data suggesting that ribosomal proteins, and perhaps ribosomes, are normally oversynthesized (1).

Autoregulation of ribosome biosynthesis has been previously reported. Defects in the yeast secretory pathway lead to the transcriptional repression of RP genes (36). Interestingly, when alterations in the secretory pathway are coupled with the depletion of a 60S RP, but not a 40S RP, the transcription of RP genes is derepressed (35, 67). Specificity in the responses to the small and large ribosomal subunits was also indicated in our studies (Fig. 3) and supports the existence of independent regulatory mechanisms targeting the 40S and 60S ribosomal subunits. The identification of separate molecular machineries involved in the biogenesis and nuclear export of the small and large ribosomal subunits is consistent with this view (19, 56). Little is known about the molecular circuitry implicated in monitoring defective or misassembled ribosomal subunits in

eukaryotes. Several factors involved in proteasome-mediated protein degradation are important for ribosome biogenesis (16, 46, 52, 53), and subunits of the proteasome are recruited to RP genes in *Saccharomyces cerevisiae* according to genome-wide location analysis (K. Auld et al., submitted), suggesting the involvement of the proteasome in the quality control and regulation of ribosome biosynthesis.

Translational control of ribosomal protein mRNAs in yeast. Our results support the notion that in addition to transcriptional control, the expression of *S. pombe* RP mRNAs can be coordinately regulated through translational regulation. Although the mechanisms are likely to differ, eubacteria and vertebrates utilize translation as a major means of regulation for RP genes (34, 66). It seems energetically advantageous to increase the translation efficiency of 40S RP mRNAs rather than to activate a transcriptional response; an immediate translational response will circumvent the synthesis, splicing, polyadenylation, and nuclear export steps required for the generation of new transcripts.

Evidence indicates that divergent organisms use different mechanisms and *cis*-acting elements to control the translation of RP mRNAs. Mammalian RP mRNAs harbor a terminal oligopyrimidine (TOP) motif in their 5′ untranslated regions that mediates translational control under diverse growth con-

ditions (34). Such TOP sequences are not found in budding and fission yeast RP mRNAs (our unpublished data). Similarly, RP mRNAs from the slime mold *Dictyostelium* lack 5′ TOP elements but are translationally repressed during specific developmental stages (50). Further evidence supporting the posttranscriptional regulation of yeast RP mRNAs comes from experiments where mRNA decay was examined at a genome-wide level in *S. cerevisiae*. This study revealed that RP mRNAs are among the least stable messages in the cell (20), consistent with the existence of *cis*-acting determinants within yeast RP mRNAs. Our data and work by others (20, 27, 63) strongly suggest that yeast RP mRNAs are posttranscriptionally regulated at the levels of translation and stability. We were unable to identify potential *cis*-acting elements that are significantly conserved among the 5′ or 3′ untranslated regions of *S. pombe* 40S RP genes by using a variety of computational analyses. It is possible that the determinants mediating the posttranscriptional regulation of RP mRNAs are located within the coding regions, as previously suggested (22).

Interestingly, the mRNA coding for rpS2 did not respond to the translational upregulation detected for most 40S RP mRNAs in *rmt3*-null cells (Fig. 3). Our observation was confirmed by real-time PCR analysis of rpS2 mRNA across polysomal profiles of wild-type and *rmt3*Δ cells and further indicated that the rpS2 mRNA is translated more actively than other 40S RP mRNAs under normal growth conditions (data not shown). Our preliminary observations suggest a model in which rpS2 is overproduced relative to other 40S RPs and in which methylation by RMT3 modulates rpS2 activity and/or stability, thereby regulating small ribosomal subunit biosynthesis.

Role of RMT3 in regulation of ribosome biosynthesis. What is the mechanism that causes the ribosomal subunit imbalance in *rmt3*Δ cells? Although the molecular details remain to be determined, our data indicate that rpS2 overexpression restores the stoichiometry between small and large ribosomal subunits in *rmt3*-null cells. This suggests that the role of arginine methylation by RMT3 in the regulation of ribosome biosynthesis primarily influences the expression or function of rpS2. Interestingly, *rmt3* is one of the *S. pombe* core environmental stress response genes that are downregulated in response to three or more stress conditions (13). Therefore, the reduction of 40S ribosomal subunit levels upon repression of *rmt3* expression (Fig. 5A), coupled with the coordinate transcriptional and translational downregulation of RP genes during stress (27, 41, 49), could represent a stress-dependent mechanism activated alongside the phosphorylation of eukaryotic initiation factor 2 (23) to downregulate translation initiation by limiting the number of available free 40S ribosomal subunits.

Together with recent studies (7, 43, 49), our findings highlight translation as an important layer of gene regulation and emphasize the importance of accounting for the translational response when analyzing signaling pathways using genomic approaches. Further characterization of RMT3 in the regulation of ribosome biosynthesis and of the signaling pathways involved in ribosomal subunit autoregulation will be important given recent findings that indicate that many RP genes are haploinsufficient tumor suppressors (2, 54) and that ribosome synthesis is an important determinant of cell size (25, 33).

REFERENCES

1. **Abovich, N., L. Gritz, L. Tung, and M. Rosbash.** 1985. Effect of RP51 gene dosage alterations on ribosome synthesis in *Saccharomyces cerevisiae*. Mol. Cell. Biol. **5:**3429–3435.
2. **Amsterdam, A., K. C. Sadler, K. Lai, S. Farrington, R. T. Bronson, J. A. Lees, and N. Hopkins.** 2004. Many ribosomal protein genes are cancer genes in zebrafish. PLoS Biol. **2:**E139.
3. **Ashburner, M., C. A. Ball, J. A. Blake, D. Botstein, H. Butler, J. M. Cherry, A. P. Davis, K. Dolinski, S. S. Dwight, J. T. Eppig, M. A. Harris, D. P. Hill, L. Issel-Tarver, A. Kasarskis, S. Lewis, J. C. Matese, J. E. Richardson, M. Ringwald, G. M. Rubin, and G. Sherlock.** 2000. Gene ontology: tool for the unification of biology. The Gene Ontology Consortium. Nat. Genet. **25:**25–29.
4. **Bachand, F., and P. A. Silver.** 2004. PRMT3 is a ribosomal protein methyltransferase that affects the cellular levels of ribosomal subunits. EMBO J. **23:**2641–2650.
5. **Bedford, M. T., and S. Richard.** 2005. Arginine methylation, an emerging regulator of protein function. Mol. Cell **18:**263–272.
6. **Berriz, G. F., O. D. King, B. Bryant, C. Sander, and F. P. Roth.** 2003. Characterizing gene sets with FuncAssociate. Bioinformatics **19:**2502–2504.
7. **Blais, J. D., V. Filipenko, M. Bi, H. P. Harding, D. Ron, C. Koumenis, B. G. Wouters, and J. C. Bell.** 2004. Activating transcription factor 4 is translationally regulated by hypoxic stress. Mol. Cell. Biol. **24:**7469–7482.
8. **Boisvert, F. M., C. A. Chenard, and S. Richard.** 2005. Protein interfaces in signaling regulated by arginine methylation. Sci. STKE **2005:**re2.
9. **Boisvert, F. M., J. Cote, M. C. Boulanger, and S. Richard.** 2003. A proteomic analysis of arginine methylated protein complexes. Mol. Cell. Proteomics **2:**1319–1330.
10. **Boisvert, F. M., U. Dery, J. Y. Masson, and S. Richard.** 2005. Arginine methylation of MRE11 by PRMT1 is required for DNA damage checkpoint control. Genes Dev. **19:**671–676.
11. **Causton, H. C., B. Ren, S. S. Koh, C. T. Harbison, E. Kanin, E. G. Jennings, T. I. Lee, H. L. True, E. S. Lander, and R. A. Young.** 2001. Remodeling of yeast genome expression in response to environmental changes. Mol. Biol. Cell **12:**323–337.
12. **Chen, D., H. Ma, H. Hong, S. S. Koh, S. M. Huang, B. T. Schurter, D. W. Aswad, and M. R. Stallcup.** 1999. Regulation of transcription by a protein methyltransferase. Science **284:**2174–2177.
13. **Chen, D., W. M. Toone, J. Mata, R. Lyne, G. Burns, K. Kivinen, A. Brazma, N. Jones, and J. Bahler.** 2003. Global transcriptional responses of fission yeast to environmental stress. Mol. Biol. Cell **14:**214–229.
14. **Dez, C., and D. Tollervey.** 2004. Ribosome synthesis meets the cell cycle. Curr. Opin. Microbiol. **7:**631–637.
15. **Eisen, M. B., P. T. Spellman, P. O. Brown, and D. Botstein.** 1998. Cluster analysis and display of genome-wide expression patterns. Proc. Natl. Acad. Sci. USA **95:**14863–14868.
16. **Fatica, A., M. Oeffinger, M. Dlakic, and D. Tollervey.** 2003. Nob1p is required for cleavage of the 3′ end of 18S rRNA. Mol. Cell. Biol. **23:**1798–1807.
17. **Gary, J. D., and S. Clarke.** 1998. RNA and protein interactions modulated by protein arginine methylation. Prog. Nucleic Acid Res. Mol. Biol. **61:**65–131.
18. **Gasch, A. P., P. T. Spellman, C. M. Kao, O. Carmel-Harel, M. B. Eisen, G. Storz, D. Botstein, and P. O. Brown.** 2000. Genomic expression programs in the response of yeast cells to environmental changes. Mol. Biol. Cell **11:**4241–4257.
19. **Granneman, S., and S. J. Baserga.** 2004. Ribosome biogenesis: of knobs and RNA processing. Exp. Cell Res. **296:**43–50.
20. **Grigull, J., S. Mnaimneh, J. Pootoolal, M. D. Robinson, and T. R. Hughes.** 2004. Genome-wide analysis of mRNA stability using transcription inhibitors and microarrays reveals posttranscriptional control of ribosome biogenesis factors. Mol. Cell. Biol. **24:**5534–5547.
21. **Henry, M. F., and P. A. Silver.** 1996. A novel methyltransferase (Hmt1p) modifies poly(A)$^+$-RNA-binding proteins. Mol. Cell. Biol. **16:**3668–3678.
22. **Herrick, D., R. Parker, and A. Jacobson.** 1990. Identification and comparison of stable and unstable mRNAs in *Saccharomyces cerevisiae*. Mol. Cell. Biol. **10:**2269–2284.
23. **Holcik, M., and N. Sonenberg.** 2005. Translational control in stress and apoptosis. Nat. Rev. Mol. Cell Biol. **6:**318–327.

24. Jakovljevic, J., P. A. de Mayolo, T. D. Miles, T. M. Nguyen, I. Leger-Silvestre, N. Gas, and J. L. Woolford, Jr. 2004. The carboxy-terminal extension of yeast ribosomal protein S14 is necessary for maturation of 43S preribosomes. Mol. Cell 14:331–342.

25. Jorgensen, P., I. Rupes, J. R. Sharom, L. Schneper, J. R. Broach, and M. Tyers. 2004. A dynamic transcriptional network communicates growth potential to ribosome synthesis and critical cell size. Genes Dev. 18:2491–2505.

26. Kressler, D., J. de la Cruz, M. Rojo, and P. Linder. 1997. Fal1p is an essential DEAD-box protein involved in 40S-ribosomal-subunit biogenesis in *Saccharomyces cerevisiae*. Mol. Cell. Biol. 17:7283–7294.

27. Kuhn, K. M., J. L. DeRisi, P. O. Brown, and P. Sarnow. 2001. Global and specific translational regulation in the genomic response of *Saccharomyces cerevisiae* to a rapid transfer from a fermentable to a nonfermentable carbon source. Mol. Cell. Biol. 21:916–927.

28. Kwak, Y. T., J. Guo, S. Prajapati, K. J. Park, R. M. Surabhi, B. Miller, P. Gehrig, and R. B. Gaynor. 2003. Methylation of SPT5 regulates its interaction with RNA polymerase II and transcriptional elongation properties. Mol. Cell 11:1055–1066.

29. Lee, S. W., S. J. Berger, S. Martinovic, L. Pasa-Tolic, G. A. Anderson, Y. Shen, R. Zhao, and R. D. Smith. 2002. Direct mass spectrometric analysis of intact proteins of the yeast large ribosomal subunit using capillary LC/FTICR. Proc. Natl. Acad. Sci. USA 99:5942–5947.

30. Loar, J. W., R. M. Seiser, A. E. Sundberg, H. J. Sagerson, N. Ilias, P. Zobel-Thropp, E. A. Craig, and D. E. Lycan. 2004. Genetic and biochemical interactions among Yar1, Ltv1 and Rps3 define novel links between environmental stress and ribosome biogenesis in Saccharomyces cerevisiae. Genetics 168:1877–1889.

31. Louie, D. F., K. A. Resing, T. S. Lewis, and N. G. Ahn. 1996. Mass spectrometric analysis of 40S ribosomal proteins from Rat-1 fibroblasts. J. Biol. Chem. 271:28189–28198.

32. Lyne, R., G. Burns, J. Mata, C. J. Penkett, G. Rustici, D. Chen, C. Langford, D. Vetrie, and J. Bahler. 2003. Whole-genome microarrays of fission yeast: characteristics, accuracy, reproducibility, and processing of array data. BMC Genomics 4:27.

33. Marygold, S. J., C. M. Coelho, and S. J. Leevers. 2005. Genetic analysis of RpL38 and RpL5, two minute genes located in the centric heterochromatin of chromosome 2 of Drosophila melanogaster. Genetics 169:683–695.

34. Meyuhas, O. 2000. Synthesis of the translational apparatus is regulated at the translational level. Eur. J. Biochem. 267:6321–6330.

35. Miyoshi, K., R. Tsujii, H. Yoshida, Y. Maki, A. Wada, Y. Matsui, E. A. Toh, and K. Mizuta. 2002. Normal assembly of 60S ribosomal subunits is required for the signaling in response to a secretory defect in Saccharomyces cerevisiae. J. Biol. Chem. 277:18334–18339.

36. Mizuta, K., and J. R. Warner. 1994. Continued functioning of the secretory pathway is essential for ribosome synthesis. Mol. Cell. Biol. 14:2493–2502.

37. Odintsova, T. I., E. C. Muller, A. V. Ivanov, T. A. Egorov, R. Bienert, S. N. Vladimirov, S. Kostka, A. Otto, B. Wittmann-Liebold, and G. G. Karpova. 2003. Characterization and analysis of posttranslational modifications of the human large cytoplasmic ribosomal subunit proteins by mass spectrometry and Edman sequencing. J. Protein Chem. 22:249–258.

38. Ong, S. E., G. Mittler, and M. Mann. 2004. Identifying and quantifying in vivo methylation sites by heavy methyl SILAC. Nat. Methods 1:119–126.

39. Pawlak, M. R., C. A. Scherer, J. Chen, M. J. Roshon, and H. E. Ruley. 2000. Arginine N-methyltransferase 1 is required for early postimplantation mouse development, but cells deficient in the enzyme are viable. Mol. Cell. Biol. 20:4859–4869.

40. Pearson, N. J., H. M. Fried, and J. R. Warner. 1982. Yeast use translational control to compensate for extra copies of a ribosomal protein gene. Cell 29:347–355.

41. Preiss, T., J. Baron-Benhamou, W. Ansorge, and M. W. Hentze. 2003. Homodirectional changes in transcriptome composition and mRNA translation induced by rapamycin and heat shock. Nat. Struct. Biol. 10:1039–1047.

42. Ptushkina, M., N. Malys, and J. E. McCarthy. 2004. eIF4E isoform 2 in Schizosaccharomyces pombe is a novel stress-response factor. EMBO Rep. 5:311–316.

43. Rajasekhar, V. K., A. Viale, N. D. Socci, M. Wiedmann, X. Hu, and E. C. Holland. 2003. Oncogenic Ras and Akt signaling contribute to glioblastoma formation by differential recruitment of existing mRNAs to polysomes. Mol. Cell 12:889–901.

44. Rudra, D., Y. Zhao, and J. R. Warner. 2005. Central role of Ifh1p-Fhl1p interaction in the synthesis of yeast ribosomal proteins. EMBO J. 24:533–542.

45. Sasaki, T., E. A. Toh, and Y. Kikuchi. 2000. Yeast Krr1p physically and functionally interacts with a novel essential Kri1p, and both proteins are required for 40S ribosome biogenesis in the nucleolus. Mol. Cell. Biol. 20:7971–7979.

46. Schafer, T., D. Strauss, E. Petfalski, D. Tollervey, and E. Hurt. 2003. The path from nucleolar 90S to cytoplasmic 40S pre-ribosomes. EMBO J. 22:1370–1380.

47. Schawalder, S. B., M. Kabani, I. Howald, U. Choudhury, M. Werner, and D. Shore. 2004. Growth-regulated recruitment of the essential yeast ribosomal protein gene activator Ifh1. Nature 432:1058–1061.

48. Shen, E. C., M. F. Henry, V. H. Weiss, S. R. Valentini, P. A. Silver, and M. S. Lee. 1998. Arginine methylation facilitates the nuclear export of hnRNP proteins. Genes Dev. 12:679–691.

49. Smirnova, J. B., J. N. Selley, F. Sanchez-Cabo, K. Carroll, A. A. Eddy, J. E. McCarthy, S. J. Hubbard, G. D. Pavitt, C. M. Grant, and M. P. Ashe. 2005. Global gene expression profiling reveals widespread yet distinctive translational responses to different eukaryotic translation initiation factor 2B-targeting stress pathways. Mol. Cell. Biol. 25:9340–9349.

50. Steel, L. F., and A. Jacobson. 1987. Translational control of ribosomal protein synthesis during early *Dictyostelium discoideum* development. Mol. Cell. Biol. 7:965–972.

51. Swiercz, R., M. D. Person, and M. T. Bedford. 2005. Ribosomal protein S2 is a substrate for mammalian PRMT3 (protein arginine methyltransferase 3). Biochem. J. 386:85–91.

52. Tabb, A. L., T. Utsugi, C. R. Wooten-Kee, T. Sasaki, S. A. Edling, W. Gump, Y. Kikuchi, and S. R. Ellis. 2001. Genes encoding ribosomal proteins Rps0A/B of Saccharomyces cerevisiae interact with TOM1 mutants defective in ribosome synthesis. Genetics 157:1107–1116.

53. Tone, Y., and E. A. Toh. 2002. Nob1p is required for biogenesis of the 26S proteasome and degraded upon its maturation in Saccharomyces cerevisiae. Genes Dev. 16:3142–3157.

54. Torok, I., D. Herrmann-Horle, I. Kiss, G. Tick, G. Speer, R. Schmitt, and B. M. Mechler. 1999. Down-regulation of RpS21, a putative translation initiation factor interacting with P40, produces viable minute imagos and larval lethality with overgrown hematopoietic organs and imaginal discs. Mol. Cell. Biol. 19:2308–2321.

55. Tsay, Y. F., J. R. Thompson, M. O. Rotenberg, J. C. Larkin, and J. L. Woolford, Jr. 1988. Ribosomal protein synthesis is not regulated at the translational level in Saccharomyces cerevisiae: balanced accumulation of ribosomal proteins L16 and rp59 is mediated by turnover of excess protein. Genes Dev. 2:664–676.

56. Tschochner, H., and E. Hurt. 2003. Pre-ribosomes on the road from the nucleolus to the cytoplasm. Trends Cell Biol. 13:255–263.

57. Tusher, V. G., R. Tibshirani, and G. Chu. 2001. Significance analysis of microarrays applied to the ionizing radiation response. Proc. Natl. Acad. Sci. USA 98:5116–5121.

58. Wade, J. T., D. B. Hall, and K. Struhl. 2004. The transcription factor Ifh1 is a key regulator of yeast ribosomal protein genes. Nature 432:1054–1058.

59. Warner, J. R., G. Mitra, W. F. Schwindinger, M. Studeny, and H. M. Fried. 1985. *Saccharomyces cerevisiae* coordinates accumulation of yeast ribosomal proteins by modulating mRNA splicing, translational initiation, and protein turnover. Mol. Cell. Biol. 5:1512–1521.

60. Warner, J. R., J. Vilardell, and J. H. Sohn. 2001. Economics of ribosome biosynthesis. Cold Spring Harbor Symp. Quant. Biol. 66:567–574.

61. Wu, C. C., M. J. MacCoss, G. Mardones, C. Finnigan, S. Mogelsvang, J. R. Yates III, and K. E. Howell. 2004. Organellar proteomics reveals Golgi arginine dimethylation. Mol. Biol. Cell 15:2907–2919.

62. Yadav, N., J. Lee, J. Kim, J. Shen, M. C. Hu, C. M. Aldaz, and M. T. Bedford. 2003. Specific protein methylation defects and gene expression perturbations in coactivator-associated arginine methyltransferase 1-deficient mice. Proc. Natl. Acad. Sci. USA 100:6464–6468.

63. Yin, Z., S. Wilson, N. C. Hauser, H. Tournu, J. D. Hoheisel, and A. J. Brown. 2003. Glucose triggers different global responses in yeast, depending on the strength of the signal, and transiently stabilizes ribosomal protein mRNAs. Mol. Microbiol. 48:713–724.

64. Yoon, H. J., and T. F. Donahue. 1992. The sui1 suppressor locus in *Saccharomyces cerevisiae* encodes a translation factor that functions during tRNA(iMet) recognition of the start codon. Mol. Cell. Biol. 12:248–260.

65. Yu, M. C., F. Bachand, A. E. McBride, S. Komili, J. M. Casolari, and P. A. Silver. 2004. Arginine methyltransferase affects interactions and recruitment of mRNA processing and export factors. Genes Dev. 18:2024–2035.

66. Zengel, J. M., and L. Lindahl. 1994. Diverse mechanisms for regulating ribosomal protein synthesis in Escherichia coli. Prog. Nucleic Acid Res. Mol. Biol. 47:331–370.

67. Zhao, Y., J. H. Sohn, and J. R. Warner. 2003. Autoregulation in the biosynthesis of ribosomes. Mol. Cell. Biol. 23:699–707.